Biogeosciences Discuss., https://doi.org/10.5194/bg-2017-351
Manuscript under review for journal Biogeosciences
Discussion started: 13 September 2017

Intense pCO_2 and $[O_2]$ Oscillations in a Mussel-Seagrass Habitat: Implications for Calcification.

Vincent Saderne[1,2], Peer Fietzek[1,3], Jens Daniel. Müller[4], Arne Körtzinger[1,5] and Claas Hiebenthal[1]

[1]{GEOMAR Helmholtz Centre for Ocean Research Kiel, Kiel, Germany}

[2]{KAUST King Abdullah University of Science and Technology, Thuwal, Kingdom of Saudi Arabia}

[3]{Kongsberg Maritime Contros GmbH, Kiel, Germany}

[4]{Leibniz Institute for Baltic Sea Research, Warnemünde, Germany}

[5]{Christian Albrecht University, Kiel, Germany}

Correspondence to: V. Saderne (vincent.saderne@KAUST.edu.sa)

Abstract

Numerous studies have been conducted on the effect of ocean acidification on calcifiers inhabiting nearshore benthic habitats, such as the blue mussel *Mytilus edulis*. The majority of these experiments was performed under stable CO_2 partial pressure (pCO_2), carbonate chemistry and oxygen (O_2) levels, reflecting present or expected future open ocean conditions. Consequently, levels and variations occurring in coastal habitats, due to biotic and abiotic processes, were mostly neglected, even though these variations largely override global long-term trends. To highlight this hiatus and guide future research, state-of-the-art technologies were deployed to obtain high-resolution time series of pCO_2 and $[O_2]$ on a mussel patch within a *Zostera marina* seagrass bed, in Kiel Bay (western Baltic Sea) in August and September 2013. Combining the in situ data with results of discrete sample measurements, a full seawater carbonate chemistry was derived using statistical models. An average pCO_2 more than 50% (~640 µatm) higher than current atmospheric levels was found right above the mussel patch. Diel amplitudes of pCO_2 were large: 765 ± 310 (mean ± SD). Corrosive conditions for calcium carbonates (Ω_{arag} and $\Omega_{calc} < 1$) centered on sunrise

were found, but the investigated habitat never experienced hypoxia throughout the study period. It is estimated that mussels experience conditions limiting calcification for 12 - 15 h per day, based on a regional calcium carbonate concentration physiological threshold. Our findings call for more extensive experiments on the impact of fluctuating corrosive conditions on mussels. We also stress the complexity of the interpretation of carbonate chemistry time series data in such dynamic coastal environments.

1 Introduction

Since preindustrial times, the atmospheric CO_2 mixing ratio rose from approximately 280 ppmv to actual ~400 ppm (Mauna Loa, annual mean 2016, NOAA-ESRL). Future climate scenarios predict a strong further increase of up to 1000 ppm by the year 2100 (IPCC, 2013). The dissolution of anthropogenic CO_2 in seawater causes an increase in the seawater CO_2 partial pressure (pCO_2) and a concurrent decrease of the seawater pH, a global phenomenon also referred to as ocean acidification (OA) (Bates et al., 2014 and Doney et al., 2009).

OA reduces the supersaturation of seawater with respect to calcite and aragonite, which may cause seawater to become corrosive for these calcium carbonates, that compose the shells and skeletons of marine species (see Harvey et al., 2013 and Andersson et al., 2011 for review and meta-analysis). In their review, Wahl et al. (2015) counted a total of 350 studies on the response of benthic marine fauna and flora to ocean acidification, either in the field or in mesocosms. The majority of these studies considered open ocean pH and pCO_2 as reference for the scenarios employed to study the impact of OA. Indeed, the carbonate system (pH, pCO_2, dissolved inorganic carbon (DIC) and total alkalinity (TA)) in surface oceans is understood relatively well, and many models exist predicting the future rise of pCO_2 and decrease of pH (e.g. Orr et al., 2005). However, very recent articles highlight the inapplicability of these predictions for the nearshore environment (Duarte et al., 2013; Wahl et al., 2015; Müller et al., 2016) and the serious lack of relevant datasets for the different major types of benthic habitats worldwide (Wahl et al., 2015). In addition to OA, ocean warming and eutrophication of coastal waters around the world cause a spreading and shoaling of hypoxia ($[O_2] < 60$ µmol kg^{-1}) in the ocean's interior (Diaz and Rosenberg, 2008; Keeling et al., 2010).

In nearshore areas, metabolic processes by flora and fauna (photosynthesis, respiration and calcification) and redox reactions in the sediment (e.g. sulfate reduction/sulfide oxidation, denitrification/nitrification) strongly affect the carbonate chemistry of the water column, temporarily generating strong disequilibria for CO_2 and O_2 between the sea and the atmosphere. Cycles of super- and undersaturation for these two metabolic gases have been observed in all kinds of benthic habitats at daily and seasonal scale, but also in relation to physical forcing such as tides, wind or precipitation (Hofmann et al., 2011; Saderne et al., 2013; see Wahl et al., 2015 for review).

As an example, in the western Baltic Sea (Eckernförde Bay) Saderne et al. (2013) found daily variations of pCO_2 of 200 - 400 µatm between July and September in a macrophyte meadow dominated by the brown algae *Fucus serratus*, with maximum pCO_2 levels reaching up to approximately 2200 µatm during upwelling conditions. As a consequence, seawater saturation states for calcite and aragonite (Ω_{calc} and Ω_{arag}) repeatedly fell below the dissolution threshold ($\Omega < 1$, i.e. seawater turning undersaturated and hence corrosive to these biominerals) during the upwelling event, which was monitored over several days.

Here, we present a case study of a mixed seagrass/mussel bed, illustrating the carbonate chemistry conditions typically experienced by calcifiers in their natural habitat. We measured pCO_2 and dissolved oxygen ($[O_2]$) directly above a mussel patch of less than 2 m² extension, surrounded by seagrass, in a mosaic seagrass-mussel habitat as it is characteristic for western Baltic Sea nearshore benthic habitats. We used a combination of autonomous in situ sensors for pCO_2, $[O_2]$, salinity and temperature, complemented by discrete sampling for DIC, TA, phosphate, and silicate, for a period of more than 7 weeks in summer 2013. Using statistical modeling, we derived time series for the entire study period for carbonate chemistry parameters including Ω_{calc} and Ω_{arag}. Based on literature knowledge regarding effects of carbonate ion concentration ($[CO_3^{2-}]$) as well as Ω_{calc} and Ω_{arag} effects on mussel biomineralization, we identified time windows of potentially favorable and unfavorable conditions for mussel calcification.

2. Materials and Methods

2.1 Description of Kiel Bay and the experimental site

Kiel Bay is a narrow and shallow bay in the western Baltic Sea that consists of two basins. The inner Kiel Bay (see Fig. 1A) in the south is up to approximately 2 km wide and (except for a few deeper dips) up to 14 m deep, while the outer Kiel Bay is up to approximately 5 km wide and approximately 20 m deep and opens in the north to the larger Kiel Bight (Kögler and Ulrich, 1985; Schwarzer and Themann, 2003). Surface and bottom water bodies of the larger Kiel Bight swash in and out Kiel Bay (mainly driven by varying wind directions and intensities). Freshwater influx from the small river "Schwentine" (east side of Kiel Bay, opposite to GEOMAR on Fig. 1A) also shapes the hydrology of the inner Kiel Bay. The strict separation of deep and shallow water bodies by stratification in the larger Kiel Bight and its bays that typically occurs during summer months is occasionally broken-up by wind-driven upwelling. The shallow coastal communities are then put in contact with high CO_2 and sometimes hypoxic sub-surface waters (Feely et al., 2008; Melzner et al., 2013).

In Kiel Bay, as in several other enclosed bays of the western Baltic Sea, the blue mussel *Mytilus edulis* and the seagrass *Zostera marina* co-occur in patches forming mosaic habitats (Reusch and Chapman, 1995; Vinther et al., 2008; Vinther and Holmer 2008; Vinther et al. 2012). A sensor package measuring pCO_2, $[O_2]$, salinity and temperature was deployed at 2 m depth in a mixed habitat formed by *Z. marina* and *M. edulis* in Kiel Bay, western Baltic Sea (54.3467 °N, 10.1539 °E; see Fig.1A). The package was directly placed on a mussel patch within the seagrass bed. The deployment was conducted for 50 days from the 08.08.2013 to 27.09.2013 with short power interruptions from 10.08., 17:10 to 11.08., 8:00 and from 12.08., 5:00 to 14.08., 16:00.

2.2 *In situ* sensor suite

Temperature, salinity and $[O_2]$ were measured simultaneously every 10 min with a SBE 37–SI MicroCAT (temperature and salinity, Sea-Bird Electronics Inc., USA) and an oxygen optode Aanderaa 3835 (Aanderaa Data Instruments AS, Norway) enclosed in a flow cell. The circulation of water between the SBE 37–SI and the optode was achieved by means of an SBE 5M pump (Sea.-Bird Electronics Inc., USA) that ran for 30 seconds every 10 min. The coordination of pumping and recording by the SBE 37 and the optode was carried out by a custom-made data logger (Todd Martz Laboratory, Scripps Institution of Oceanography, San Diego, USA). To prevent fouling on sensors, the SBE 37–SI was equipped with tributyltin tablets and copper tubing linked the SBE 37–SI and the flow cell to the pump.

A HydroC® CO_2 II sensor (KM Contros GmbH, Kiel, Germany) was used to autonomously measure in situ CO_2 partial pressure (pCO_2). The sensor determines pCO_2 optically by means of an nondispersive infrared (NDIR) absorption measurement within a membrane-equilibrated headspace (Fietzek et al., 2014). The sensor was calibrated at a water temperature of 17.5 °C at 6 different pCO_2 levels across a measurements range of 200 - 2200 µatm by the manufacturer before (July) and after (November) the measurements. The corresponding calibration polynomials had a quality of R^2 = 0.999998 and 0.99998 with root mean square errors of 1.15 and 3.98 ppm. Calibrations and data processing were carried out according to Fietzek et al. (2014) with the exception that, here, the interpolation between the pre- and the post-deployment calibration polynomial was carried out according to the sensor's absolute run-time between the two calibrations.

During the field deployment, the sensor was powered from the nearby pier. Data were stored internally on its data logger. The sensor was configured to carry out a 2 min zeroing every 6 h. A flushing interval duration of 55 min was used to analyze the data during recovery from zero to ambient values. During the subsequent measurement interval, a 10 s mean of the 1 Hz raw data was stored every minute.

The HydroC® was equipped with a flow-head allowing for passive diffusion of seawater to the sensor's membrane through a circumferential orifice along the cylindrical sensor housing. In order to improve the data quality under the given configuration and deployment conditions, determination and correction of the sensor's response time (RT) were given special attention (see Appendix A for further information). The sensor's in situ RT was determined to be 546 ± 208 s (mean ± SD) and the final pCO_2 series was response time corrected assuming a constant RT of 546 s.

We conclude a general uncertainty for the final pCO_2 series in this study of 2.5% of reading as the standard deviation of the pCO_2 measurements. This value is comprised of the accuracy of drift corrected HydroC® pCO_2 data of approximately 1% of reading as found within Fietzek et al. (2014) and the uncertainty estimate of 1.5% of reading related to the actual RT influences (see Appendix A).

2.3 Discrete sampling

Biogeosciences Discuss., https://doi.org/10.5194/bg-2017-351
Manuscript under review for journal Biogeosciences
Discussion started: 13 September 2017

Over the course of the deployment, a total of 31 seawater samples for DIC and TA were taken at the sensor suite through snorkeling. Sampling was conducted twice a week in the hours following sunrise and solar noon. On a third day, duplicate sampling was conducted in the hour following solar noon. Corresponding sampling results were averaged to improve the quality of the measurements. Salinity of the water samples was measured in a laboratory at GEOMAR using a conductometer (SG 7/8, Mettler Toledo, Switzerland). Subsequently, the samples were poisoned with mercury chloride following the recommendations by Dickson et al. (2007). DIC (precision ± 3 µmol kg^{-1}) was measured by coulometry using a SOMMA instrument (University of Rhode Island, USA) and TA (precision ± 6 µmol kg^{-1}) was determined with a VINDTA titrator (Marianda GmbH, Germany) following Dickson et al. (2007).

In parallel to all DIC and TA samplings, another set of seawater samples was taken and frozen for measurement of phosphate and silicate concentrations. Total phosphate (precision 0.1 µmol kg^{-1}) and total silicate (precision 0.2 µmol kg^{-1}) concentrations were measured using a QuAAtro auto-analyzer with an XY-2 sampler (SEAL Analytical GmbH, Germany).

2.4.1 Correction for Organic Alkalinity

The pCO_2 in the discrete sample was calculated from measured DIC, TA, total phosphate and total silicate using the first and second carbonate system dissociation constants for brackish waters from Millero (2006) and the dissociations constants of HF and HSO_4^- of Perez and Fraga (1987) and Dickson (1990), respectively, with the R package Seacarb (Lavigne and Gattuso, 2013).

A critical point for the calculation of carbonate chemistry in waters containing significant amounts of dissolved organic matter, in the following referred to as DOC, is the contribution of organic acid-base components to the TA (Cai et al., 1998; Kuliński et al., 2014 and Yang et al., 2015). This organic TA contribution (TA_{org}) is not reflected in models employed to interpret titration data nor in equations routinely used to perform carbonate system calculations. The classical concept, i.e. two out of four measureable carbonate system parameters are sufficient to calculate the remaining, is limited if TA is one of the measured parameters and the sample contains high amounts of DOC. In such cases, the TA value determined by titration can significantly exceed the amount of TA contributed by the inorganic acid-base components. This hinders an accurate quantification of the inorganic alkalinity and thereby affects the calculation of other carbonate system parameters.

Kuliński et al. (2014) demonstrated that the pCO_2 calculated from TA and DIC is typically 100 - 200 µatm lower than the measured pCO_2 in open waters of the Baltic Sea. This deviation is not observed if pCO_2 is calculated from measured DIC and pH data (Fig. 2), which are unaffected by the TA_{org} contribution. Two aspects of the present study therefore require the consideration of TA_{org}: (i) TA_{org} explains the observed differences between pCO_2 measured in situ and pCO_2 calculated from DIC, TA, silicate and phosphate of discrete samples (Fig. 2) and (ii) TA_{org} needs to be considered when other carbonate system parameters (pH_T, DIC, Ω_{arag} and Ω_{calc}) are calculated from the TA and pCO_2 time series.

The offset between measured and calculated pCO_2 caused by TA_{org} increases towards higher pCO_2 levels. This could be repeatedly observed during another measuring campaign in Kiel Bay (Hiebenthal et al., 2017, Fig. 2). To furthermore unravel the difference in observed versus calculated pCO_2 for typical Kiel Bay conditions (S = 16, T = 18 °C, DOC = 300 µmol kg^{-1}, TA = 1950 µmol kg^{-1}), we qualitatively reproduced the impact of TA_{org} on the carbonate system by a modelling approach using regional TA_{org} properties reported by Kuliński et al. (2014). Our modelling approach revealed an offset between measured and observed pCO_2 that increases with CO_2 partial pressure and reaches up to 300 µatm at pCO_2 levels around 2000 µatm (Fig. 2, solid line). A more detailed description of the modelling approach is given in Appendix B.

For the calculation of carbonate system parameters (pH, DIC, Ω_{arag} and Ω_{calc}) from TA and pCO_2 data, we consequently corrected the TA time series originally based on titration measurements for a TA_{org} contribution. Therefore we used 18 discrete seawater samples taken at 1 m depth right next to a constantly deployed HydroC® CO_2 sensor at GEOMAR pier in the inner Kiel Bay, 2 km south of the above described experimental site between March and December 2015 (Hiebenthal et al., 2017). The water samples were poisoned with $HgCl_2$ (Dickson et al., 2007) within 15 min and stored until measurement of DIC, pH_T and TA at the Leibniz Institute for Baltic Sea Research, Warnemünde, Germany. DIC was analyzed with a SOMMA system at 15 °C. TA was determined by an open-cell titration at 20 °C. Certified reference materials provided by Andrew Dickson's laboratory were measured in parallel for quality assurance. The pH_T of each water sample was determined spectrophotometrically at 25 °C with unpurified m-cresol purple as indicator dye (Hammer et al., 2014). Phosphate and silicate concentrations used for the 2015 samples were

measure after Grasshoff 1999 and sampled approximately 240 m from GEOMAR pier (Hiebenthal et al., 2017).

The TA_{org} fraction measured in Kiel inner Bay, determined as the difference between TA measured and TA calculated from DIC and pH_T, at GEOMAR pier 2015 was 0.84 ± 0.0005% (mean ± SE), corresponding to a contribution between approximately 8 and 30 µmol kg^{-1}. We chose to consider this conservative range for the carbonate chemistry calculations instead of the values determined during the 2013 deployment, 0.48 ± 0.28% (mean ± SE). The reason for using the 2015 value is that it was determined from measurements of TA, DIC and pH_T in the same water samples (Hiebenthal et al., 2017), thereby avoiding the additional uncertainty and noise in the data due to a spatio-temporal mismatch between pCO_2 sensor and discrete sample data of the 2013 field deployment.

2.5 Seawater carbonate chemistry

We used a model approach based on discrete water sample- and salinity data to estimate total alkalinity (TA) from salinity (S). Given the obvious changes particularly in phosphate and salinity around September 1st (Fig. 3A-B), two separate TA-S regressions were calculated for August and September (Fig. 4, Tab. 1). The slopes and intercepts were used to derive total alkalinity from the salinity time series. Both regressions were highly significant with p-values < 0.001, R^2 = 0.64 and 0.92 for August and September respectively and standard deviations of the residuals < 15 µmol kg^{-1} (Fig. 4). The two intercepts for August and September are notably different by 100 µmol kg^{-1} while the two slopes are similar (~40 µmol kg^{-1}). An organic-free TA range was calculated (TA_{inorg}) by subtracting constant organic alkalinity contributions of 8 and 30 µmol kg^{-1} (lower and upper TA_{org} limits in 2015 measurements at GEOMAR pier; see 2.4) from the TA time series.

2.6 Calculation of the regional atmospheric pCO_2

Half-hourly measured CO_2 mole fractions in dry air from the German Federal Environment Agency (Umweltbundesamt), Station Westerland, 8.3082 °E and 54.9250 °N, were averaged for the months August (08th – 31st 2013) and September (01st – 27th 2013): 391 ± 7 and 395 ± 14 ppm (mean ± SD). Thereof pCO_2 in wet air (100% relative humidity at SST) of 385 and 388 µatm for August and September, respectively, were derived at local measurement conditions; i.e. using an averaged sea surface temperature (18.4 ± 0.6 and 16.1 ± 1.0 °C) and ambient pressure readings

(1019.6 ± 4.2 and 1015.7 ± 7.5 mbar; both parameters from GEOMAR meteorological station, Fig. 1A) as well as the salinity measured in this study (15.6 ± 0.7 and 15.9 ± 1.0).

2.7 Inferential statistics

Daily means, maxima, minima as well as day-night peak-to-peak amplitudes and daily duration of undersaturation for calcite and aragonite (in hours) (mean ± SD) for the months of August and September were compare using Mann-Whitney U tests. Statistical analyses were conducted with Statistica 7 (Statsoft, USA).

3 Results

3.1 Salinity, water temperature, total silicate and total phosphate observations

Salinity did not show circadian patterns and the daily mean salinity was not significantly different between August and September (Mann-Whitney U, $p > 0.05$, see Appendix C for detailed statistics), with 15.65 ± 0.7 and 15.89 ± 1.01 (mean ± SD), respectively (Fig. 3A). The total alkalinity (TA), derived from salinity, varied between 1934 and1956 µmol kg^{-1} during the 2 months, with a SD of 41 µmol kg^{-1}. As a marker of seasonality, temperature daily means, minima, maxima were all significantly lower in September compared to August (Mann-Whitney U, $p < 0.001$, see Appendix C), with drops of 2.3 °C, 2.2 °C and 3 °C, respectively (Tab. 2, Fig. 3A, 4A). The daily variation amplitude was significantly reduced in September by 0.3°C compared to August (Mann-Whitney U, $p < 0.01$, see Appendix C). Total silicate was not significantly different between August and September: 19.0 ± 4.9 µmol kg^{-1} and 18.8 ± 5.4 µmol kg^{-1} (Mann-Whitney U, $p > 0.05$, see Appendix C). Total phosphate was significantly different between August and September: 0.7 ± 0.14 µmol kg^{-1} and 5.9 ± 3.7 µmol kg^{-1} (Mann-Whitney U, $p < 0.001$, see Appendix C).

3.2 pCO_2 and $[O_2]$ observations

The daily mean (± SD) pCO_2 of 628 ± 114 µatm in August and 652 ± 193 µatm in September (Tab. 2) remained always above the regional atmospheric pCO_2 of approximately 387 µatm. The mean daily minimum and maximum pCO_2 values were 334 ± 119 µatm and 1151 ± 328 µatm in August and 373 ± 139 µatm and 1097 ± 336 µatm (mean ± SD) in September, respectively (see Tab. 2,

Figs. 3C, 5B). A modest and non-significant increase of the daily means was observed between August and September (+ 22 µatm) as well as a non-significant average decrease of the day-night variability by 93 µatm (Mann-Whitney U, $p > 0.05$, see Appendix C) (Tab. 2). A high pCO_2 event was observed between September 8th and September 12th with a peak of the daily mean pCO_2 to 1166 µatm on September 9th. On this day, a maximum pCO_2 of 1839 µatm was observed at 04:30 a.m. (see Fig. 3C).

The daily mean [O_2] most of the time remained below the seawater saturation threshold (~260 to 290 µmol kg^{-1}) (Fig. 3D, Tab. 2). However, supersaturation due to photosynthesis was regularly observed between noon and sunset in August. Significant decreases of the daily average, maximum and minimum [O_2] by 47 µmol kg^{-1}, 64 µmol kg^{-1}, 35 µmol kg^{-1}, respectively, were observed in September (Mann-Whitney U, all $p < 0.001$, see Appendix C for details) (Tab. 2, Fig. 5C), with an abrupt [O_2] decrease occurring on Sept. 8th, in parallel to a sudden decrease in temperature by approximately 2 °C (Fig. 3A-D). A significant decrease of the day-night amplitude by 29 µmol kg^{-1} was observed from August to September (Mann-Whitney U, $p = 0.008$, Appendix C). The threshold for hypoxia (60 µmol kg^{-1}) is never undercut (see Fig. 3D); the minimum daily mean concentration observed during the two months was 140 µmol kg^{-1}.

3.3 Derived carbonate chemistry parameters

Times series for pH_T, DIC, Ω_{arag} and Ω_{calc} (Fig. 6) were derived from modeled TA_{inorg} (Fig. 4) and measured pCO_2 and analyzed for daily means, minima, maxima and diel peak-to-peak amplitudes (mean ± SD) with TA_{org} = 8 µmol kg^{-1} and TA_{org} = 30 µmol kg^{-1} (Tab. 1). Since the differences in the calculated parameters between the TA_{org} = 8 µmol kg^{-1} and the TA_{org} = 30 µmol kg^{-1} estimates are too small to be recognizable in Fig. 6, only results for the mean TA_{org} = 19 µmol kg^{-1} are shown. Overall, we observe a slight and non-significant (Mann-Whitney U, $p > 0.05$, see Appendix C for details) decrease in daily means of DIC and pH_T between August and September by 11 µmol kg^{-1} and 0.02 pH_T units respectively (Tab. 1). In parallel, we observe a non-significant decrease of the amplitudes of the diel variations in DIC of 21 µmol kg^{-1} (Mann-Whitney U, $p > 0.05$, see Appendix C) and pH_T of approximately 0.05 pH_T units (Mann-Whitney U, $p > 0.05$, see Appendix C) and (Tab. 1, Fig. 5). All these observations are coherent with the changes in pCO_2 previously described.

Daily means of Ω_{arag} are close to the saturation threshold: between 1.3 and 1.4 in August and 1.2 in September (Tab. 1). For both, Ω_{arag} and Ω_{calc}, we observe a significant decrease in daily mean values (Mann-Whitney U, all $p < 0.01$, see Appendix C) and a marginally significant decrease of diel amplitudes between August and September (Mann-Whitney U, all $p < 0.1$, see Appendix C) (Tab. 1, Fig. 5). In both isoforms, the amplitudes decrease results from a significant reduction of the daily maxima (Mann-Whitney U, $p = 0.001$, see Appendix C) with the minima remaining constant (Mann-Whitney U, $p > 0.05$, see Appendix C) (Tab. 1, Fig. 5). On average, the seawater was undersaturated with respect to aragonite for approximately 6 hours per days in August and approximately 9 hours per day in September (Tab. 1). Similarly, seawater was undersaturated with respect to calcite for approximately 30 min and approximately 1 hour 30 min in August and September, respectively (Tab. 1). Only one full day of undersaturation with respect to aragonite was observed on September 9th during the high pCO_2 event (Fig. 5).

Over the whole measurement period, the consideration of organic alkalinity contributions has little effect on the derived CO_2 system parameters (mean value differences: 20 µmol kg^{-1} DIC, < 2 µmol kg^{-1} [CO_3^{2-}] and negligible effect on omegas and pH_T). The only noticeable difference when taking TA_{org} into account was an increase of time of undersaturation for Ω_{arag} and Ω_{calc} in September of approximately 25 min and approximately 10 min, respectively.

4 Discussion

4.1 pCO_2, carbonate chemistry and O_2

Monthly averages of pCO_2 close to the seafloor as presented in this study (~640 µatm; Tab. 1) were more than 50% above atmospheric pCO_2. In 2011, Saderne et al. (2013), used similar technologies as in our study in a seaweed dominated bed of Eckernförde Bay (adjacent to Kiel Bay, Western Baltic) and found significantly lower weekly mean pCO_2 values (~390 µatm in July, ~240 µatm in August and 420 µatm in September, excluding an upwelling event, Saderne et al., 2013). Accordingly, the day-night amplitudes of pCO_2 observed in the present study (764 ± 310 µatm, overall mean ± SD) are 3 to 4 times higher than observed during "normal" days by Saderne et al. (2013) (243 ± 95 µatm) in the neighboring Eckernförde Bay in 2011. This reflects a characteristic of the marine carbonate system: Equal DIC variations will induce stronger pCO_2 variations at high "baseline" pCO_2 levels compared to lower pCO_2 levels. The source of this pattern

is the reduced buffering capacity of the carbonate system at a high pCO_2 "baseline". Accordingly, Saderne et al. (2013) found extreme pCO_2 variations of approximately 1700 µatm during an upwelling event that lifted the "baseline" pCO_2 to approximately 1600 µatm, although the DIC variations due to plant photosynthesis remained rather unchanged by the upwelling. Likewise, the amplitude of the diel DIC variations during our study (145 µmol kg^{-1} in August and 124 µmol kg^{-1} in September, see Tab.1 and Fig. 5) were of the same magnitude as what had been observed in Eckernförde Bay before and after upwelling (141 µmol kg^{-1} and 106 µmol kg^{-1}, respectively,Saderne et al., 2013).

Average O_2 concentrations were below saturation in August and September 2013, with a significant decrease occurring in September (monthly means of 89.4% $[O_2]_{sat}$ and 68.8% $[O_2]_{sat}$ for August and September respectively). However, we note that at no point of our survey the threshold of hypoxia (~22% saturation; 60 µmol kg^{-1}) was reached.The significant O_2 decrease in September co-occurred with an increase in phosphate and a change in DIC to TA regression. This can possibly be explained by a rapid degradation of the seagrass shouts observed in September and a possible shift of the habitat from an auto- to a heterotrophic system.

4.2 Implications for mussel calcification in a seagrass meadow

We found pronounced variations of Ω_{calc} and Ω_{arag} on a daily basis, e.g., resulting in 5.7 to 8.8 h of undersaturation for aragonite per day in the water body right above the mussel patch.

As expected, daytime photosynthesis counters water corrosiveness caused by heterotrophic processes, while at night water corrosiveness is reinforced by respiration. Waldbusser et al. (2014) demonstrated that saturation states (and therefore $[CO_3^{2-}]$) are the parameters affecting the larval development and growth of *Mytilus galloprovincialis* and *Crassostrea gigas*. On young *M. edulis* Hiebenthal et al. (2013) found a negative correlation between growth and Ω or $[CO_3^{2-}]$. Thomsen et al. (2015) confirmed these findings in larvae and juveniles. With a meta-analysis including all past work on mussel populations from Kiel Bay, they found that the critical CO_3^{2-} concentration below which calcification starts to decline was 80 µmol kg^{-1} (although they specified that the directly related ratio $[H^+]/[HCO_3^-]$ is likely to be the controlling parameter for calcification, Thomsen et al. 2015). In our survey, mussels were exposed to $[CO_3^{2-}]$ below this threshold for 12 ± 5.2 h per day in August and 15.3 ± 5.4 h per day in September (mean ± SD). Comparing these

findings to the shorter durations of aragonite (5-9 h per day) and calcite (~1 h per day) undersaturation implies that reduced calcification rates might already occur during periods with low, yet oversaturated calcium carbonate concentrations. However, the consequences of these successions of intense corrosive stress and stress relaxation on the juvenile and adults forming the mussel patch is still under debate. On mussel larvae, Frieder et al., 2013 showed that the negative effects of elevated pCO_2 (~1500 µatm) on *Mytilus galloprovincialis* disappear, if diel variations of 500 µatm were added, although this effect was not observed for *Mytilus californianus*. Wahl et al. (2017) found that in laboratory and mesocosm experiments calcification of blue mussels is significantly higher during daytime, when photosynthetic activity of macrophytes creates favorable calcification conditions. However, in field studies they did not detect a positive net effect of the co-occurrence with macrophytes on the calcification of mussels (Wahl et al. 2017). Furthermore, Thomsen et al. (2013) showed that high food availability, particularly in Kiel Bay, can circumvent the effects of acidification in mussels.

Conclusion

Our study demonstrates how essential it is to place more effort in measuring the carbonate chemistry variations in nearshores habitats, and highlights the need to include variability when investigating the impact of OA on benthic organisms. We emphasize that continuous carbonate system observations in benthic habitats are possible but challenging due to the high spatio-temporal variability and organic alkalinity contributions. However, with the here applied combination of in situ sensor measurements, laboratory analyses of discrete water samples, and modelling elements we were able to distinguish daily oscillations and shifts of averages (across weeks) of several seawater chemistry parameters. This approach specifically allowed for a temporal quantification of dissolution threshold undercuts *M. edulis* experiences in this exemplary site of Kiel Bay.

Appendix A: HydroC® response time and related signal processing

The entire HydroC® pCO_2 time series has a total of 187 zeroings and related flush intervals. A first order kinetics model was fitted to every of the HydroC®'s signal recoveries from its zero value to ambient partial pressure over an 55 min flush interval to obtain sensor response times (see Fiedler

et al. 2013). The fit interval was set to extend over 55 min to be around 6 times as large as the sensor's response time to allow for reasonable fitting of the exponential increase. In general the carbonate system at the site was characterized by a strongly varying baseline featuring very steep pCO_2 gradients over the course of the day with slopes of up to -54 µatm/min. Therefore the pCO_2 signal recovery from zero to ambient during the 187 flush intervals was often superimposed with a changing background partial pressure. These adverse conditions hamper the response time determination by means of a first order kinetics fit. We therefore flagged and not considered further the recoveries providing the worst fit results, which indicates a bad match between model and real signal: (i) the fits characterized by the largest 10% of root mean square (RMS) residuals of the fitted curve and the real signal as well as (ii) the fits with the largest 10% of the uncertainty of the fitted response time.

Finally a total of 157 fit results were considered providing an average response time (t_{63}) of 546 ± 208 s with an RMS of the fit function of 6.0 ± 3.1 µatm and a fit uncertainty for the response time of 1.2 ± 0.4 s. The average response time found is in good agreement with a t_{63} of 553 ± 8 µatm as determined during a dedicated laboratory test with a similar sensor setup at 14.5°C water temperature. The large standard deviation of the averaged in situ response times (i.e. 208 s) is likely caused (i) by the influence of the strongly varying background pCO_2 on the data to be fitted and (ii) by the variability of the water exchange in front of the membrane within the flow-head as caused by i.e. changes in the ambient water currents. Against the large variability in the determined response times, a temperature dependence of the t_{63} can be neglected as well as a potential response deceleration caused by fouling on the membrane, which was only observed to a very small extend after the deployment.

The response time (RT) correction according to Miloshevich et al. (2004) and Fiedler et al. (2013) was carried out with a constant response time of 546 s to obtain the final pCO_2 series. The pCO_2 data were additionally RT-corrected with a reduced (RT_{short} = 546 – 208 = 338 s) and an extended response time (RT_{long} = 546 + 208 = 754 s). In order to estimate the uncertainty of the final pCO_2 time series, the differences between the RT_{long}- and the RT-corrected as well as between the RT- and the RT_{short}-corrected pCO_2 time series were determined. They both provide a small average ΔpCO_2 of 0.8 µatm (0.06% of reading) and a corresponding standard deviation of 10 µatm (1.5% of reading). The standard deviation is influenced by short periods characterized by large pCO_2 gradients where the RT-correction has the largest effect; i.e. at 130 µatm/min over 3 minutes

(54 µatm/min in the original, non-RT-corrected data) the steepest pCO_2 decline of the series was observed in the early morning of August 22nd at around 4:40 causing the maximum observed individual ΔpCO_2 of -172 µatm or 23% of reading.

The standard deviation of the ΔpCO_2 (1.5% of reading) is used as a measure for the pCO_2 uncertainty in this study related to the response time influences. Not considering the response time and applying a related correction, would have forced us to continue the analysis with a less realistic, "smoothed" data set that showed temporally delayed as well as amplitude-damped pCO_2 peaks and troughs.

Fiedler, B., Fietzek, P., Vieira, N., Silva, P., Bittig, H. C. and Körtzinger, A.: In Situ CO_2 and O_2 Measurements on a Profiling Float, J. Atmos. Ocean. Technol., 30(1), 112–126, doi:10.1175/JTECH-D-12-00043.1, 2013.

Miloshevich, L. M., Paukkunen, A., Vömel, H. and Oltmans, S. J.: Development and validation of a time-lag correction for Vaisala radiosonde humidity measurements, J. Atmos. Ocean. Technol., 21(9), 1305–1327, 2004.

Appendix B

We implemented a model to estimate the potential error associated to CO_2 system calculations, in case one of the input parameters is titrated TA including organic acid-base components.

Hence, we firstly calculated the carbonate system at varying DIC and constant TA, salinity, and temperature. In this case the derived carbonate system parameters (i.e. pCO_2) reflect values as calculated from TA and DIC measured in discrete samples.

Organic contribution to TA (TA_{org}) is estimated based on the relation reported by Kuliński et al. (2014) for the Baltic Sea, which approximates TA_{org} from the proton concentration $[H^+]$, the amount of DOC, a bulk dissociation constant (K_{DOM}) and the fraction of DOC (f) acting as a carrier of weakly acidic groups

$$TA_{org} = \frac{K_{DOM} \cdot f \cdot DOC}{[H^+] + K_{DOM}}$$

This TA_{org} estimate is a side-specific approximation since K_{DOM} and f (2.94×10^{-8} mol kg^{-1} and 0.14, respectively) are characteristic for the actual DOM composition. Further, K_{DOM} is currently only reported for T=25°C and no salinity-dependence was investigated. Therefore, this model is only a qualitative approximation of the carbonate system in high DOC waters.

The inorganic TA fraction can be approximated as $TA_{inorg} = TA - TA_{org}$. This TA_{inorg} together with DIC can be used to calculate the "correct" pCO_2 ($pCO_{2,sensor}$) as it would also be obtained from direct observations, since TA_{inorg} represents the share of the alkalinity which is covered by the dissociation constants and equilibrium reactions implemented in the routinely applied carbonate system models (i.e. CO_2sys, seacarb).

Finally, the TA_{org} estimate needs to be refined. Above, it was estimated from the proton concentration, which itself was derived from TA and DIC. Now, TA_{inorg} is the better input parameter to calculate this proton concentration. Thus, we recalculate first TA_{org} to get a refined value ($TA_{org,ref}$). The other carbonate system parameters, including $pCO_{2,sensor,ref}$, are calculated with $TA_{org,ref}$. This refinement procedure was repeated iteratively, until no significant changes occurred between the iterative steps. The finally obtained $pCO_{2,sensor,ref}$ would reflect direct pCO_2 measurements performed with a dedicated in situ sensor.

Model output:

The model predicts an increase in the deviation between pCO_2 measured in situ ($pCO_{2,sensor,ref}$) and pCO_2 values obtained by calculations from discrete sample TA and DIC towards pCO_2 levels around 2000 µatm as depicted in Fig. 2 (input parameters: S = 16, T = 18 °C, DOC = 300 µmol kg^{-1}, TA = 1950 µmol kg^{-1}, K_{DOM} and *f* from Kuliński et al. (2014), CO_2 system constants from Millero et al. (2006)).

Kuliński, K., Schneider, B., Hammer, K., Machulik, U. and Schulz-Bull, D.: The influence of dissolved organic matter on the acid–base system of the Baltic Sea, J. Mar. Syst., 132, 106–115, doi:10.1016/j.jmarsys.2014.01.011, 2014.

Millero, F. J., Graham, T. B., Huang, F., Bustos-Serrano, H. and Pierrot, D.: Dissociation constants of carbonic acid in seawater as a function of salinity and temperature, Mar. Chem., 100(1-2), 80–94, doi:10.1016/j.marchem.2005.12.001, 2006.

Appendix C: Mann-Whitney U tests details

Result table for the Mann Whitney tests comparing August and September data listed in Table 2.

	U	Z	p-value	August n	September n
Mean Temperature	2	5.71	<0.01	20	26
Min. Temperature	5	5.64	<0.01	20	26
Max. Temperature	1	5.73	<0.01	20	26
ΔTemperature	133	2.80	0.01	20	26

Mean Salinity	198	-1.36	0.17	20	26
Min. Salinity	196	-1.41	0.16	20	26
Max. Salinity	186	-1.63	0.10	20	26
ΔSalinity	252	-0.17	0.87	20	26
Total Silicate	114	0.100	0.920	13	18
Total Phosphate	0	-4.665	<0.001	13	18
Mean pCO_2	255	0.10	0.92	20	26
Min. pCO_2	220	-0.88	0.38	20	26
Max. pCO_2	233	0.59	0.56	20	26
ΔpCO_2	220	0.88	0.38	20	26
Mean $[O_2]$	67	4.758	<0.001	24	26
Min. $[O_2]$	121	3.709	<0.001	24	26
Max. $[O_2]$	68	4.738	<0.001	24	26
Δ$[O_2]$	176	2.641	0.008	24	26

TA_{org} = 8

	U	Z	p-value	August n	September n
Mean pH_T	241	0.41	0.68	20	26
Min. pH_T	246	-0.30	0.76	20	26
Max. pH_T	212	1.05	0.29	20	26
ΔpH_T	215	0.99	0.32	20	26
Mean DIC	254	0.12	0.90	20	26
Min. DIC	227	-0.72	0.47	20	26
Max. DIC	203	1.25	0.21	20	26
ΔDIC	198	1.36	0.17	20	26
Mean $[CO_3^{2-}]$	172	1.94	0.05	20	26
Min. $[CO_3^{2-}]$	225	0.76	0.44	20	26
Max. $[CO_3^{2-}]$	153	2.36	0.02	20	26
Δ$[CO_3^{2-}]$	181	1.74	0.08	20	26
Mean Ω_{arag}	157	2.27	0.02	20	26
Min. Ω_{arag}	213	1.03	0.30	20	26
Max. Ω_{arag}	150	2.43	0.02	20	26
Δ Ω_{arag}	176	1.85	0.06	20	26
time Ω_{arag} <1	176	-1.85	0.06	20	26
Mean Ω_{calc}	167	2.05	0.04	20	26
Min. Ω_{calc}	215	0.99	0.32	20	26
Max. Ω_{calc}	152	2.38	0.02	20	26

Δ Ω_{calc}	178	1.81	0.07	20	26
time Ω_{calc} <1	212	-1.05	0.29	20	26
		TA_{org} = 30			
	U	Z	p-value	August n	September n
Mean pH_T	241	0.41	0.68	20	26
Min. pH_T	246	-0.30	0.76	20	26
Max. pH_T	212	1.05	0.29	20	26
ΔpH_T	215	0.99	0.32	20	26
Mean DIC	253	0.14	0.89	20	26
Min. DIC	228	-0.70	0.49	20	26
Max. DIC	203	1.25	0.21	20	26
ΔDIC	197	1.38	0.17	20	26
Mean $[CO_3^{2-}]$	172	1.94	0.05	20	26
Min. $[CO_3^{2-}]$	225	0.76	0.44	20	26
Max. $[CO_3^{2-}]$	151	2.40	0.02	20	26
Δ$[CO_3^{2-}]$	181	1.74	0.08	20	26
Mean Ω_{arag}	157	2.27	0.02	20	26
Min. Ω_{arag}	213	1.03	0.30	20	26
Max. Ω_{arag}	149	2.45	0.01	20	26
Δ Ω_{arag}	176	1.85	0.06	20	26
time Ω_{arag} <1	175	-1.87	0.06	20	26
Mean Ω_{calc}	168	2.03	0.04	20	26
Min. Ω_{calc}	214	1.01	0.31	20	26
Max. Ω_{calc}	152	2.38	0.02	20	26
Δ Ω_{calc}	178	1.81	0.07	20	26
time Ω_{calc} <1	218	-0.9	0.4	20	26

Acknowledgements

The authors would like to thank particularly Dr. Todd Martz and his team from the Scripps Institution of Oceanography (San Diego, USA) for providing the salinity / [O_2] / T° sensor package and for their precious technical assistance. We also wish to thank the Kiel Marine Organism Culture Centre (KIMOCC) of the Kiel Cluster of excellence "Future Ocean"; Sebastian Fessler from GEOMAR for the TA / DIC sample measurements; Dr. Bernd Schneider and Stefan Bücker

469 from the IOW are thanked for valuable discussions with respect to carbonate system analysis in
470 the Baltic Sea as well as for the inter comparison between TA / DIC / pH measurements; Prof.
471 Peter Herman from the NIOZ Royal Netherlands Institute for Sea Research for providing access
472 to the nutrient analyzer; Dr. Jörn Thomsen for his comments on the manuscript; the research divers
473 from GEOMAR among which are Prof. Martin Wahl, Dr. Christian Pansch, Dr. Yvonne Sawall
474 and Christian Lieberum; the personnel of the "Seebar am Seebad Düsternbrook" restaurant for
475 providing electricity to the sensors as well as the Kiel early morning nudist club for its cooperation
476 in providing access to the Seebar. This work has been funded by the Kiel Cluster of excellence
477 "Future Ocean".

478

References

Andersson, A. J., Mackenzie, F. T. and Gattuso, J.-P.: Effects of ocean acidification on benthic processes, organisms, and ecosystems, in Ocean Acidification, p. xix, 326 p., 2011.

Bates, N. R., Y. M. Astor, M. J. Church, and others. 2014. A time-series view of changing surface ocean chemistry due to ocean uptake of anthropogenic CO_2 and ocean acidification. Oceanography 27: 126–141. doi:http://dx.doi.org/10.5670/oceanog.2014.16Cai, W.-J., Y. Wang, and R. E. Hodson: Acid-Base Properties of Dissolved Organic Matter in the Estuarine Waters of Georgia, USA. Geochim. Cosmochim. Acta 62: 473–483. doi:10.1016/S0016-7037(97)00363-3, 1998.

Cai, W.-J., Wang, Y., and Hodson, R. E.: Acid-base properties of dissolved organic matter in the estuarine waters of Georgia, USA, Geochim. Cosmochim. Ac., 62, 473–483, 1998

Diaz, R. J. and Rosenberg, R.: Spreading dead zones and consequences for marine ecosystems., Science, 321(5891), 926–9, doi:10.1126/science.1156401, 2008.

Dickson, A. G.: Standard potential of the reaction: AgCl(s) + ½ H_2(g) = Ag(s) + HCl(aq), and the standard acidity constant of the ion HSO_4^- in synthetic sea water from 273.15 to 318.15 K, J. Chem. Thermodyn., 22(2), 113–127, doi:10.1016/0021-9614(90)90074-Z, 1990.

Dickson, A. G., Sabine, C. L. and Christian, J. R.: Guide to Best Practices for Ocean CO_2 Measurements, PICES spec., 2007.

Doney, S. C., V. J. Fabry, R. A. Feely, and J. A. Kleypas. 2009. Ocean Acidification: The Other CO_2 Problem. Ann. Rev. Mar. Sci. 1: 169–192. doi:10.1146/annurev.marine.010908.163834

Duarte, C. M., Hendriks, I. E., Moore, T. S., Olsen, Y. S., Steckbauer, A., Ramajo, L., Carstensen, J., Trotter, J. A. and McCulloch, M.: Is Ocean Acidification an Open-Ocean Syndrome? Understanding Anthropogenic Impacts on Seawater pH, Estuaries and Coasts, 36(2), 221–236, doi:10.1007/s12237-013-9594-3, 2013.

Feely, R. A., Sabine, C. L., Hernandez-Ayon, J. M., Ianson, D. and Hales, B.: Evidence for upwelling of corrosive "acidified" water onto the continental shelf, Science, 320, 1490-1492, 2008.

Fietzek, P., Fiedler, B., Steinhoff, T. and Körtzinger, A.: In situ quality assessment of a novel underwater pCO_2 sensor based on membrane equilibration and NDIR spectrometry, J. Atmos. Ocean. Technol., 31(1), 181–196, 2014.

Frieder, C. A., Gonzalez, J. P., Bockmon, E. E., Navarro, M. O. and Levin, L. A.: Can variable pH and low oxygen moderate ocean acidification outcomes for mussel larvae?, Glob. Chang. Biol., 1–11, doi:10.1111/gcb.12485, 2013.

Geomar, Helmholtz Center for Ocean Research Kiel. Available from: http://www.geomar.de/service/wetter/

Grasshoff, K., Kremling, K. and Ehrhardt, M.G.: Methods of Seawater Analysis (3rd Edition). VCH Publishers. 632 pp, 1999.

Hammer, K., Schneider, B., Kuliński, K. and Schulz-Bull, D. E.: Precision and accuracy of spectrophotometric pH measurements at environmental conditions in the Baltic Sea, Estuar. Coast. Shelf Sci., 146, 24–32, 2014.

Harvey, B. P., Gwynn-Jones, D. and Moore, P. J.: Meta-analysis reveals complex marine biological responses to the interactive effects of ocean acidification and warming, Ecol. Evol., 3, 1016–1030, doi:10.1002/ece3.516, 2013.

Hiebenthal, C., Philipp, E. E. R., Eisenhauer, A. and Wahl, M.: Effects of seawater pCO_2 and temperature on shell growth, shell stability, condition and cellular stress of Western Baltic Sea *Mytilus edulis* (L.) and *Arctica islandica* (L.), Mar. Biol., 160(2013), 2073–2087, doi:10.1007/s00227-012-2080-9, 2013.

Hiebenthal, C., Fietzek, P., Müller, J.D., Otto, S., Rehder, G., Paulsen, M., Stuhr, A., Clemmesen-Bockelmann, C., Melzner, F.: Kiel fjord carbonate chemistry data between 2015 (February) and 2016 (January). GEOMAR - Helmholtz Centre for Ocean Research Kiel, Pangea Dataset #876551 (DOI registration in progress), 2017.

Hofmann, G. E., Smith, J. E., Johnson, K. S., Send, U., Levin, L. A., Micheli, F., Paytan, A., Price, N. N., Peterson, B., Takeshita, Y., Matson, P. G., Crook, E. D., Kroeker, K. J., Gambi, M. C., Rivest, E. B., Frieder, C. A., Yu, P. C. and Martz, T. R.: High-frequency dynamics of ocean pH: a

multi-ecosystem comparison., PLoS One, 6(12), e28983, doi:10.1371/journal.pone.0028983, 2011.

Keeling, R. F., Körtzinger, A. and Gruber, N.: Ocean Deoxygenation in a Warming World, Ann. Rev. Mar. Sci., 2(1), 199–229, doi:10.1146/annurev.marine.010908.163855, 2010.

Kögler, F.-C. and Ulrich, J., Bodengestalten und Sedimente der Kieler Förde, Schr. Naturwiss. Ver. Schleswig-Holstein, 55, 1–33, 1985.

Kuliński, K., Schneider, B., Hammer, K., Machulik, U. and Schulz-Bull, D.: The influence of dissolved organic matter on the acid–base system of the Baltic Sea, J. Mar. Syst., 132, 106–115, doi:10.1016/j.jmarsys.2014.01.011, 2014.

Lavigne, H. and Gattuso, J.-P.: seacarb: seawater carbonate chemistry with R. R package version 2.3. 3, Software [online] Available from: http://scholar.google.com/scholar?hl=en&btnG=Search&q=intitle:seacarb:+seawater+carbonate+chemistry+with+R.+R+package+version+2.3#0, 2010.

Melzner, F., Thomsen, J., Koeve, W., Oschlies, A., Gutowska, M. A., Bange, H. W., Hansen, H. P. and Körtzinger, A.: Future ocean acidification will be amplified by hypoxia in coastal habitats, Mar. Biol., 16, 1875-1888, doi:10.1007/s00227-012-1954-1, 2012.

Millero, F. J., Graham, T. B., Huang, F., Bustos-Serrano, H. and Pierrot, D.: Dissociation constants of carbonic acid in seawater as a function of salinity and temperature, Mar. Chem., 100(1-2), 80–94, doi:10.1016/j.marchem.2005.12.001, 2006.

Müller, J. D., B. Schneider, and G. Rehder. 2016. Long-term alkalinity trends in the Baltic Sea and their implications for CO_2-induced acidification. Limnol. Oceanogr. 61: 1984–2002. doi:10.1002/LNO.10349

NOAA - ESRL, Available from: http://www.esrl.noaa.gov/gmd/ccgg/trends, 2014.

Orr, J. C., Fabry, V.J., Aumont, O., Bopp, L., Doney, S.C., Feely, R. A., Gnanadesikan, A., Gruber, N., Ishida, A., Joos, F., Key, R. M., Lindsay, K., Maier-Reimer, E., Matear, R., Monfray, P., Mouchet, A., Najjar, R.G., Plattner, G.K., Rodgers, K.B., Sabine, C.L., Sarmiento, J.L., Schlitzer, R., Slater, R.D., Totterdell, I.J., Weirig, M.F., Yamanaka, Y. and Yool, A.: Anthropogenic ocean

558 acidification over the twenty-first century and its impact on calcifying organisms, Nature, 437,
559 681-686, 2005.

560 Perez, F. F. and Fraga, F.: The pH measurements in seawater on the NBS scale, Mar. Chem., 21,
561 315–327, 1987.

562 Reusch, T. B. H. and Chapman, A. R. O.: Storm effects on eelgrass (*Zostera marina* L.) and blue
563 mussel (*Mytilus edulis* L.) beds, J. Exp. Mar. Bio. Ecol., 192(2), 257–271, doi:10.1016/0022-
564 0981(95)00074-2, 1995.

565 Saderne, V., Fietzek, P. and Herman, P. M. J.: Extreme Variations of pCO_2 and pH in a Macrophyte
566 Meadow of the Baltic Sea in Summer: Evidence of the Effect of Photosynthesis and Local
567 Upwelling, PLoS One, 8(4), e62689, doi:10.1371/journal.pone.0062689, 2013.

568 Schwarzer, K. and Themann, S.: Sediment distribution and geological buildup of Kiel Bay
569 (Western Baltic Sea), Meyniana, 55, 91-115, 2003.

570 Thomsen, J., Casties, I., Pansch, C., Körtzinger, A. and Melzner, F.: Food availability outweighs
571 ocean acidification effects in juvenile *Mytilus edulis*: laboratory and field experiments, Glob.
572 Change Biol., 19, 1017–1027, doi:10.1111/gcb.12109, 2013,

573 Thomsen, J., Haynert, K., Wegner, K. M. and Melzner, F.: Impact of seawater carbonate chemistry
574 on the calcification of marine bivalves, Biogeosciences Discuss., 12(2), 1543–1571,
575 doi:10.5194/bgd-12-1543-2015, 2015.

576 Vinther, H. F. and Holmer, M.: Experimental test of biodeposition and ammonium excretion from
577 blue mussels (*Mytilus edulis*) on eelgrass (*Zostera marina*) performance, J. Exp. Mar. Bio. Ecol.,
578 364(2), 72–79, doi:10.1016/j.jembe.2008.07.003, 2008.

579 Vinther, H. F., Laursen, J. S. and Holmer, M.: Negative effects of blue mussel (*Mytilus edulis*)
580 presence in eelgrass (*Zostera marina*) beds in Flensborg bay, Denmark, Estuar. Coast. Shelf Sci.,
581 77(1), 91–103, doi:10.1016/j.ecss.2007.09.007, 2008.

582 Vinther, H. F., Norling, P., Kristensen, P., Dolmer, P. and Holmer, M.: Effects of coexistence
583 between the blue mussel and eelgrass on sediment biogeochemistry and plant performance, Mar.
584 Ecol. Prog. Ser., 447, 139–149, doi:10.3354/meps09505, 2012.

585 Wahl M., Saderne V., Sawall Y.: How good are we at assessing ocean acidification impact in
586 coastal systems? Limitations, omissions and strengths of commonly used experimental approaches
587 with an emphasis on the neglected role of fluctuations. Mar. Freshw. Res., 2015.

588 Wahl, M., S. Schneider Covachã, V. Saderne, C. Hiebenthal, J. D. Müller, C. Pansch, and Y.
589 Sawall. 2017. Macroalgae may mitigate ocean acidification effects on mussel calcification by
590 increasing pH and its fluctuations. Limnol. Oceanogr. doi:10.1002/lno.10608

591 Waldbusser, G. G., Hales, B., Langdon, C. J., Haley, B. a., Schrader, P., Brunner, E. L., Gray, M.
592 W., Miller, C. a. and Gimenez, I.: Saturation-state sensitivity of marine bivalve larvae to ocean
593 acidification, Nat. Clim. Chang., (December 2014), doi:10.1038/nclimate2479, 2014.

594 Yang, B., R. H. Byrne, and M. Lindemuth: Contributions of organic alkalinity to total alkalinity
595 in coastal waters: A spectrophotometric approach. Mar. Chem. 176: 199–207.
596 doi:10.1016/j.marchem.2015.09.008, 2015

Fig. 1. A. Map of the inner Kiel Bay with study site and the GEOMAR station. B. Photo of the sensor suite at the measurement site.

Fig. 2. Deviation between observed and calculated pCO_2 (ΔpCO_2) as a function of observed pCO_2 illustrating the influence of TA_{org} on carbonate system determinations. Dashed lines represent linear regressions of the respective data. **Black triangles:** $\Delta pCO_2 = pCO_2$ sensor - pCO_2 (TA, DIC) for the benthic seagrass deployment of this study, n = 30. The ΔpCO_2 can be explained by a combination of the influence of an organic TA contribution of 0.49 ± 1.47% with measurement uncertainties and sampling errors (spatio-temporal mismatches). **Dark grey diamonds:** $\Delta pCO_2 = pCO_2$ sensor - pCO_2 (TA, DIC) based on corrected HydroC® measurements and discrete samples taken at GEOMAR pier in 2015 (Hiebenthal et al., 2017). DIC, TA and pH_T were measured in the same water samples. The ΔpCO_2 is due to a TA_{org} fraction of 0.84 ± 0.0005% (mean ± SD). **Grey circles:** $\Delta pCO_2 = pCO_2$ sensor - pCO_2 (DIC, pH_T), based on corrected sensor data and discrete samples taken at GEOMAR pier during the same period in 2015, n =18 (Hiebenthal et al., 2017). There is no pCO_2 dependency of the ΔpCO_2, because neither DIC nor pH_T are impacted by TA_{org}, $R^2 = 0.005$. **Solid black line**: Difference between observed and calculated pCO_2 from a model including TA_{org} contributions typical for Baltic Sea water (for details see Appendix B).

Fig. 3. Time series for observed parameters: A: Salinity (black) and temperature (grey), 10 min sampling interval B: Total phosphate (green) and silicate (red) concentration from 31 discrete sampling events at the sensor location. C: pCO_2 at 1-min measurement interval (solid line) and 24h moving average (dashed line). D: Dissolved oxygen concentration at 10-min measurement interval (solid green line) and as 24h moving average (dashed green line). Also shown is the oxygen saturation concentration calculated from the water temperature and salinity (black). The straight solid red line represents the hypoxia threshold of 60 µmol kg^{-1}.

Fig. 4. Alkalinity (TA) time series (black line) modeled from salinity using the regression equations from August and September. Grey lines represent the TA_{inorg} time series after subtraction of the organic alkalinity contribution of 8 and 30 µmol kg^{-1} from TA, respectively. Triangles (August) and dots (September) represent TA of 31 discrete samples used for the regressions. The sample from the 1st of September at 6:40 (open dot) was not considered for the regression. Insert panel: Linear regressions of TA as function of salinity in discrete samples for the months of August

in blue (n = 14) and September in red (n= 16), see Table 1 for equations and statistics. Dashed lines are 90% confidence intervals.

Fig. 5. Hourly means (○) ± standard deviation (-) for the months of August (grey) and September (black) for Temperature (A.), pCO_2 (B.) and $[O_2]$ (C.). Hourly mean ranges and maximum upper as well as minimum lower standard deviations (-) calculated using TA_{org} contributions of 8 and30 µmol kg^{-1} for pH_T (D.), DIC (E.), $[CO_3^{2-}]$ (F.), Ω_{arag} (G.) and Ω_{calc} (H.). The dissolution thresholds of the Ω values are depicted as solid red lines in panel G. and H.

Fig. 6. Derived time series of carbonate system parameters: pH_T (A),.Dissolved inorganic carbon (DIC, B.) and saturation states for aragonite (Ω_{arag}, light brown) and calcite (Ω_{calc}, dark brown) with dissolution threshold Ω = 1 (red line, C.). All time series are calculated from pCO_2 (10 min interval) and total alkalinity with a mean organic contribution of 19 µmol kg^{-1}.

Fig. 7. Carbonate ion concentration, $[CO_3^{2-}]$, calculated from pCO_2 (10 min interval) and total alkalinity with a mean organic contribution of 19 µmol kg^{-1}. The red line represents a side specific $[CO_3^{2-}]$ threshold of 80 µmol kg^{-1} below which calcification declines in mussels according to Thomsen et al., 2015.

Biogeosciences Discuss., https://doi.org/10.5194/bg-2017-351
Manuscript under review for journal Biogeosciences
Discussion started: 13 September 2017

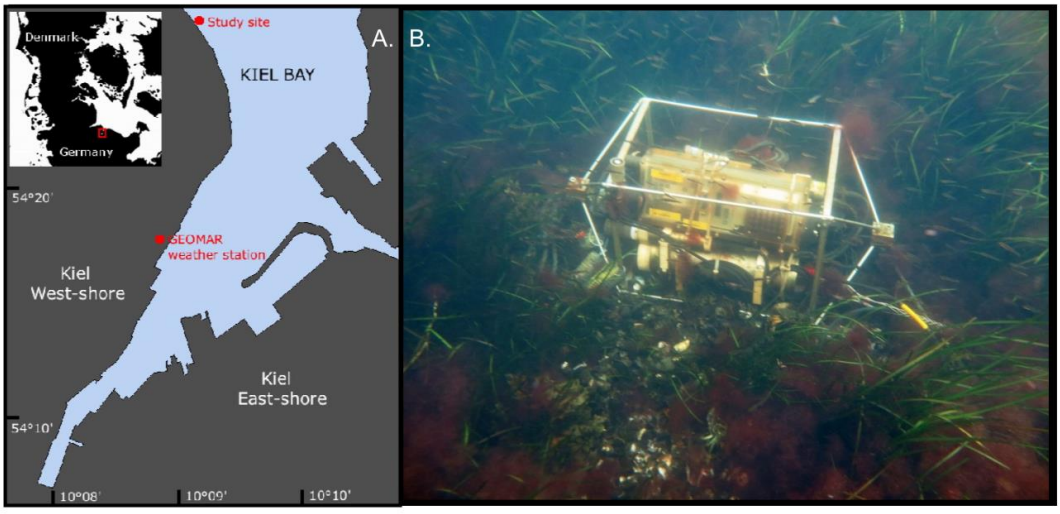

649

650

Biogeosciences Discuss., https://doi.org/10.5194/bg-2017-351
Manuscript under review for journal Biogeosciences
Discussion started: 13 September 2017

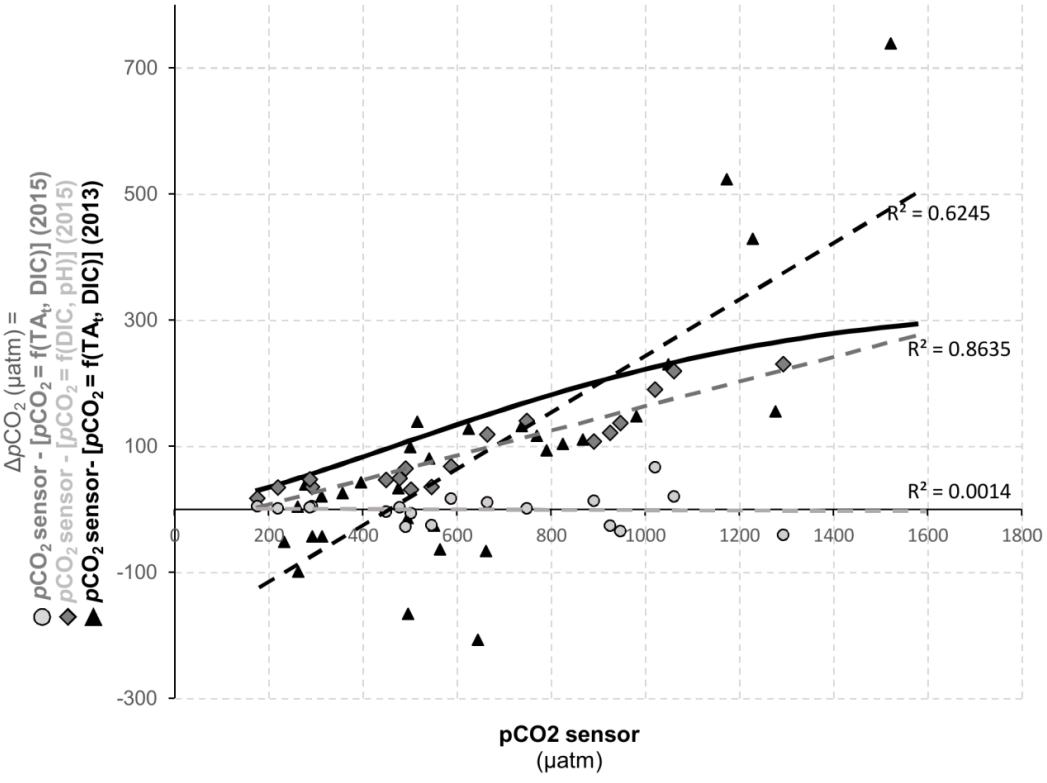

651

652

653

654

655

656

657

658

Biogeosciences Discuss., https://doi.org/10.5194/bg-2017-351
Manuscript under review for journal Biogeosciences
Discussion started: 13 September 2017

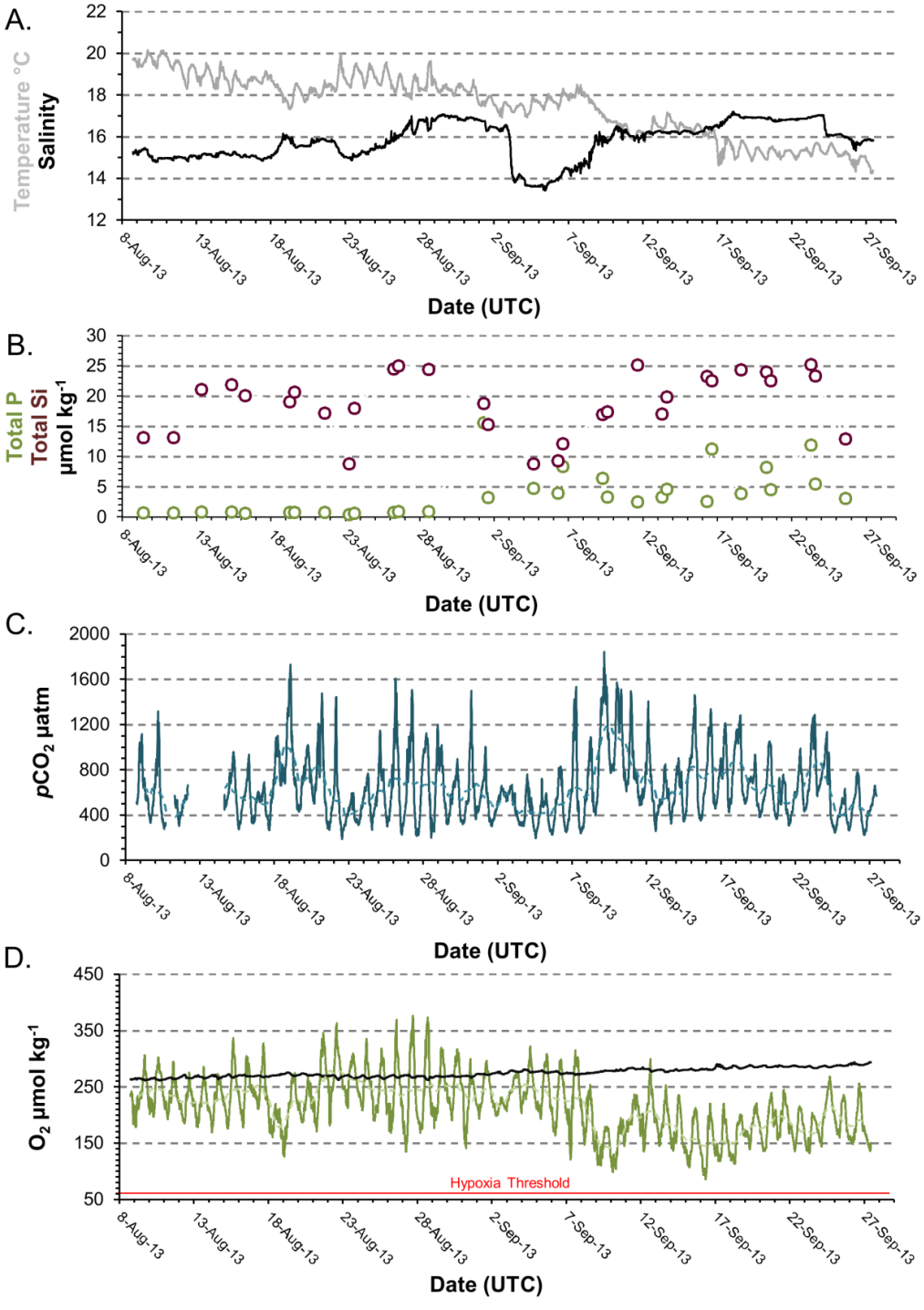

659

Biogeosciences Discuss., https://doi.org/10.5194/bg-2017-351
Manuscript under review for journal Biogeosciences
Discussion started: 13 September 2017

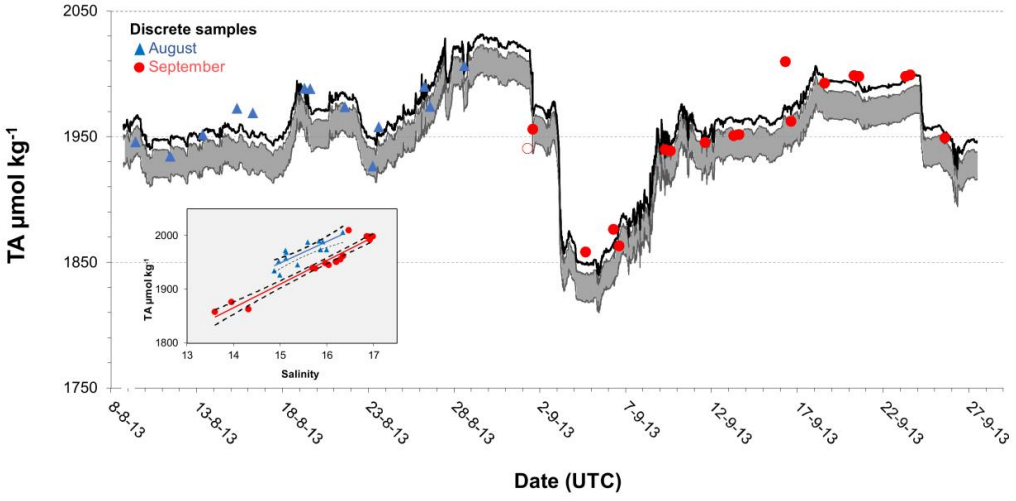

Biogeosciences Discuss., https://doi.org/10.5194/bg-2017-351
Manuscript under review for journal Biogeosciences
Discussion started: 13 September 2017

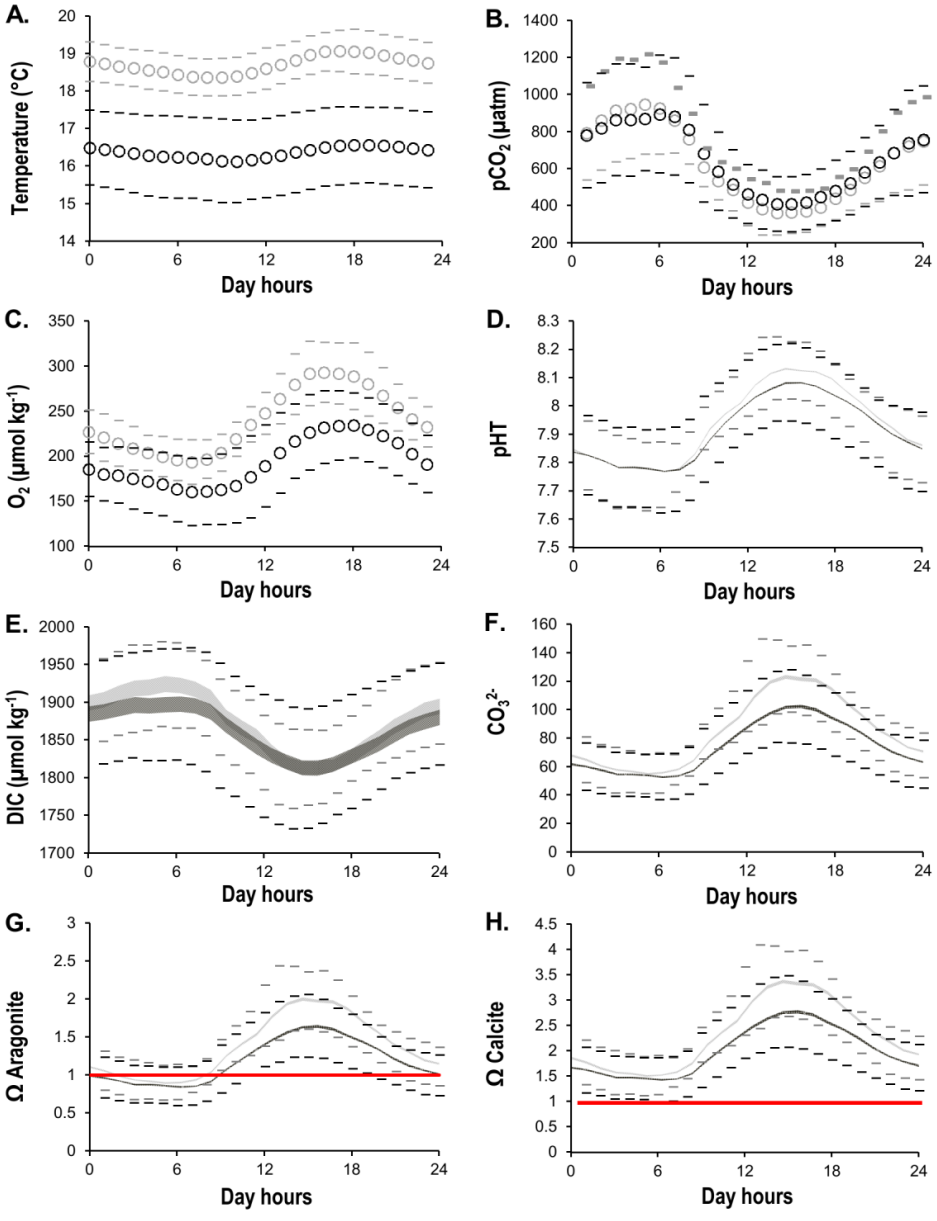

672

673

674

Biogeosciences Discuss., https://doi.org/10.5194/bg-2017-351
Manuscript under review for journal Biogeosciences
Discussion started: 13 September 2017

675

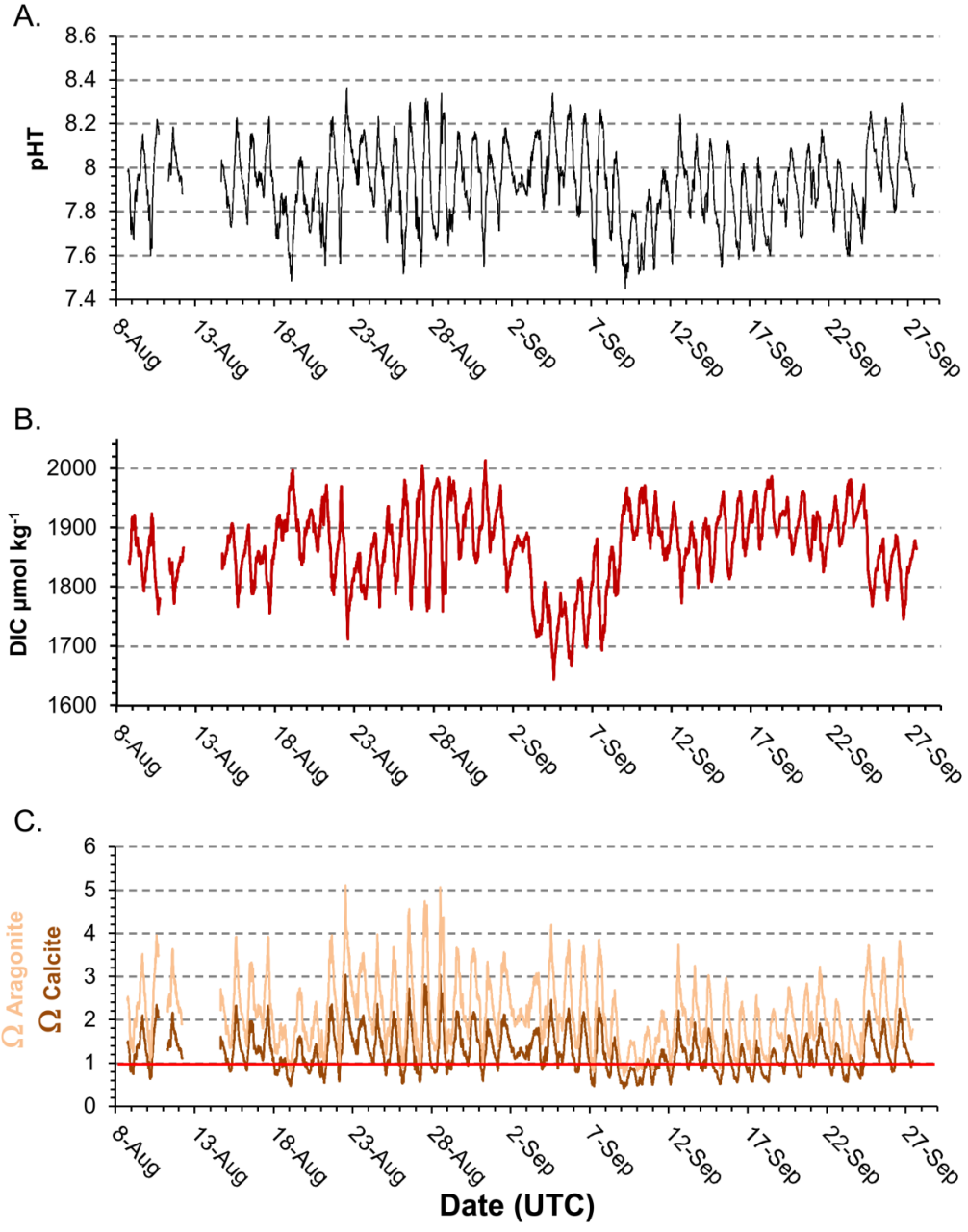

676

Biogeosciences Discuss., https://doi.org/10.5194/bg-2017-351
Manuscript under review for journal Biogeosciences
Discussion started: 13 September 2017

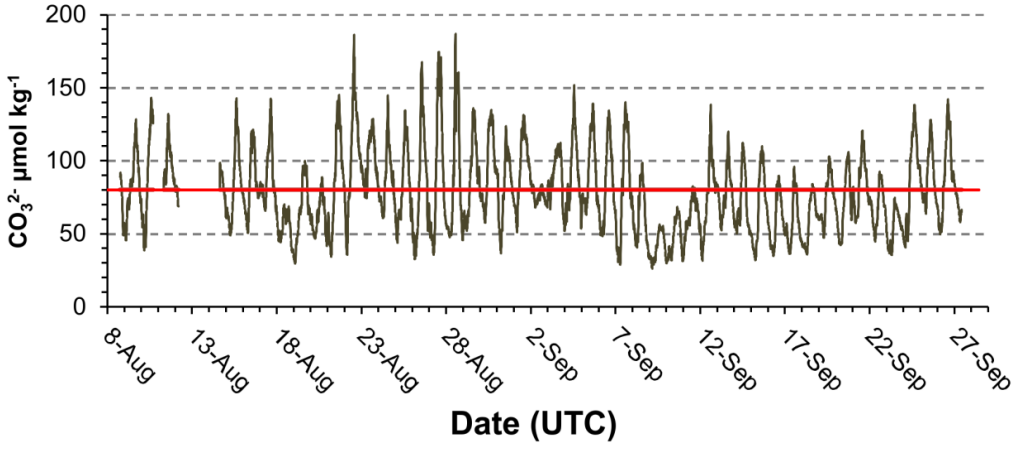

677